

Powder Blown Laser Cladding of Vertical Surfaces

P. LUBASZKA AND B. BAUFELD*

*Nuclear Advanced Manufacturing Research Centre (Nuclear AMRC),
University of Sheffield, Rotherham, Yorkshire, S60 5WG, UK*

Powder blown laser cladding is widely applied in industry to achieve functional surface modifications for corrosion or wear resistance. Commonly this is deposited in the 1G flat position in accordance to the ASME BPVC Section IX (equivalent to the ISO 6947 PA position). For certain applications, however, especially large and heavy components which are difficult to manipulate, the cladding of vertical surfaces would be beneficial – cladding in 2G horizontal position in accordance to the ASME BPVC Section IX (equivalent to the ISO 6947 PC position). The task of cladding vertical surfaces requires a specially designed cladding head. The aim of this report is to present those initial results observed through depositing powder in this attitude using a high power diode laser (HPDL). It was observed that the change of the position of the cladded surface from flat to horizontal or vertical affects the cladding process. The reason for this is that gravity affects the powder stream and weld pool in a different way. An optimized parameter set for the 1G (PA) cladding resulted in inferior clads with extensive dilution leading to inhomogeneous properties within the clad; therefore a specific cladding parameter set for the 2G (PC) position had to be developed. Different laser beam sizes and cladding parameters were investigated with the aim of achieving well bonded, crack-free overlapping beads with minimal dilution. The results indicate that the amount of transport gas and the position of a laser head critically influence the clad quality and that generally a smaller laser spot gives better results.

Keywords: High power diode laser (HPDL), stainless steel, nozzle, laser cladding, powder blown, dilution, corrosion resistance, hardness

1 INTRODUCTION

Cladding is one technology available for surface modification of components to optimize their functionality; for example, stainless steel or Ni-based alloys

*Corresponding author: Tel: +44 (0)114 222 9919; E-mail: b.baufeld@namrc.co.uk

can be utilized for corrosion resistance, while Stellite and WC alloys can be utilized for wear resistance or hard facing [1-3]. In cladding, one or more layers of a material with desired key properties, such as corrosion resistance, is applied on a surface of another material (high strength or construction steels) with full metallurgical bonding. Sufficient heat must be provided to melt a thin layer of the substrate and the clad material at the same time. Once the melt pool solidifies, a functional layer is created.

Cladding processes are utilized in many fields of the industry [4], including the nuclear industry (pressure vessels), power generation (boiler pipes), oil and gas (drilling heads), mining/tunnelling/dredging (trenching tools, conveyor screws), the food industry and many others. A number of different cladding technologies are available, including plasma transferred arc cladding, submerged arc cladding and laser cladding. The properties and quality of a cladding may differ, depending on the cladding technology; for example, arc-based technologies often exhibit significant dilution and thermal distortion [4].

Powder blown laser cladding on the other hand is characterized by high power density, low heat input and high heating and cooling rates [2,4,5] resulting in low dilution, chemical composition of the clad material achieved within few micrometres and limited thermal distortion of the workpiece due to low heat input [6,7].

Cladding in the downhand position (1G ASME/PA ISO 6947 [8]) is the most frequently used method of laser cladding. In this configuration the clad surface of the component is positioned and maintained in the flat position. But, for some applications, especially for large and heavy components, this is difficult or even impossible to achieve. The manipulation of such components may be extremely expensive and technically challenging. In particular, the tilting of rotating high-mass components at high peripheral speeds may be inherently dangerous since a difficult-to-control gyroscope is created.

These problems may be overcome by applying a set up where vertical walls are clad with the laser beam in horizontal orientation. One version would be with horizontal tracks (2G ASME/PC ISO 6947 [8]), another version would be with up- or downwards tracks (3G ASME/PF or PG ISO 6947[8]). Few commercially available cladding nozzles are capable of achieving this type of cladding and, to the authors' knowledge nothing has been published in the open literature.

IWS Fraunhofer has developed a nozzle (COAX12) for which it is claimed that the nozzle inclination does not influence the powder supply [9,10]. This nozzle applies powder injection by creating four separated powder streams which form a homogeneous powder stream that is directed onto the working point [9] and is almost unaffected by gravity. The aim of this paper is to report results obtained using this COAX12 nozzle for 2G (PC) cladding.

2 EXPERIMENTAL DETAILS

2.1 Material specifications

Carbon steel S355 plates with dimensions of $300 \times 300 \times 30 \text{ mm}^3$ were utilized for all of the experiments as a substrate. Modified stainless steel 308L powder (Carpenter Powder Products) with particles sizes of 40 to $150 \mu\text{m}$ diameter was used as the clad material. Typical chemical compositions of both materials are given in Table 1.

2.2 Laser cladding apparatus and arrangement

The laser used for the cladding was a 15.0 kW high power diode laser (HPDL) (LDF15000; Laserline, GmbH), emitting a multimode beam in a wavelength in the range of 900 to 1070 nm. A processing head (OTS2; Laserline, GmbH) a nozzle (COAX12; IWS Fraunhofer), and a 5-axis robot (KUKA Robotics Corporation) attached to a gantry (Güdel, GmbH) were deployed to create a laser cladding system. Figure 1 shows the process head oriented for 2G (PC) cladding.

Two different optical configurations were used with calculated HPDL beam diameters of 9.0 and 7.0 mm. Figure 2 shows the powder nozzle and the four powder streams oriented for cladding a vertical surface. A focus and power monitor (Primes, GmbH) was used to verify both profile and power of the laser beam.

2.3 Sample analysis procedures

The clad specimens were prepared for the analysis in accordance with the following procedure: cross sectioning by water-cooled cutting wheel; mounting in bracket for grinding; grinding by sandpaper up to 1200 mesh; and polishing with diamond liquid up to $3 \mu\text{m}$.

The first step of the analysis was macro observation of the cross-sections on an automated digital optical microscope (Smartzoom; Carl Zeiss AG) at magnifications in the range of $30\times$ to $40\times$. Clad lift and penetration depth were measured using a Zeiss software tool. The first three tracks of each sample are not representative, so were not taken into consideration during measurements.

The hardness of clad material, heat affected zone (HAZ), overlap areas and substrate material were measured applying the HV 0.1 Vickers Microhardness method using a microhardness tester (Wilkinson, Ltd.).

TABLE 1
Typical chemical composition (wt.%) of the modified 308L powder and the carbon steel S355 substrate.

Material	C	Mn	P	S	Si	Ni	Cr	Mo	Nb	Ti	Fe
308L	0.003	1.320	0.005	0.01	0.44	10.48	19.87	2.230	0.050	0.050	64.910
S355	0.160	1.490	<0.010	0.005	0.19	0.020	0.010	<0.010	0.040	<0.010	98.000

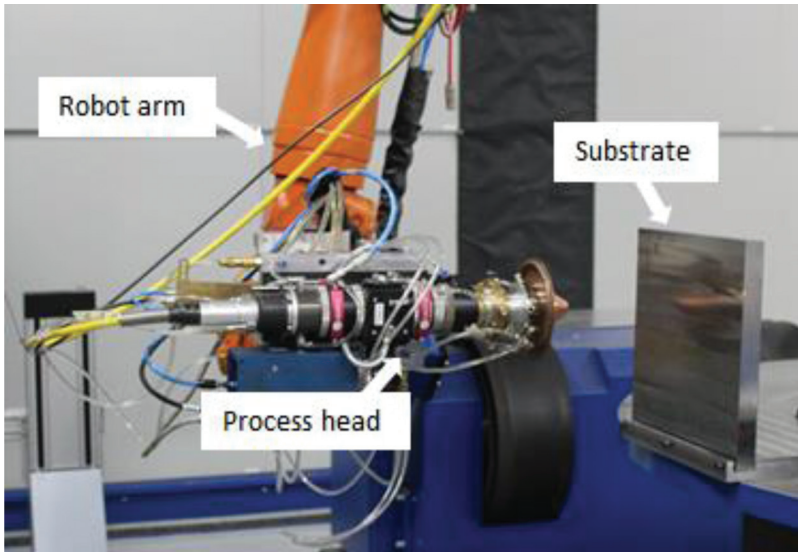


FIGURE 1
Photographic view of the arrangement for 2G powder blown HPDL cladding showing the robot arm, the process head and a substrate.

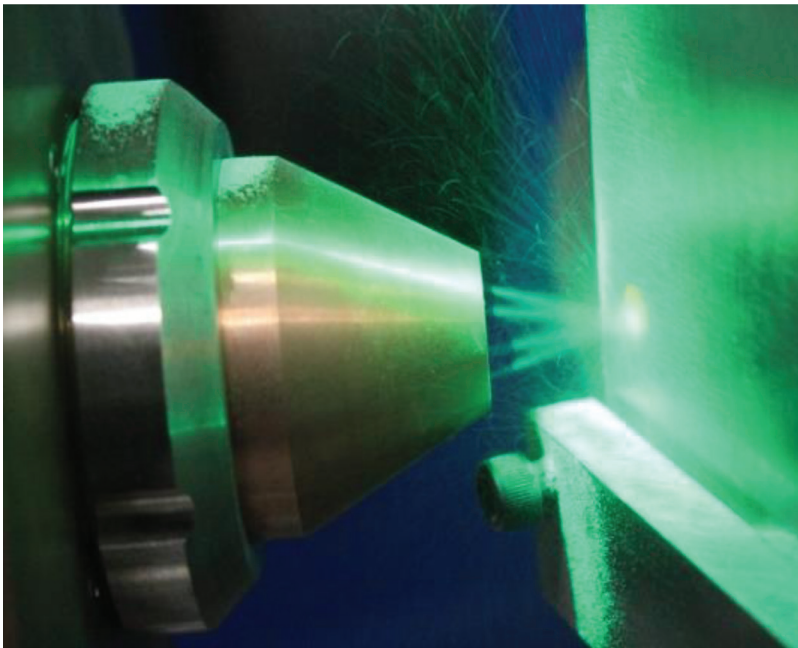


FIGURE 2
Photographic view of the COAX12 powder nozzle exhibiting the powder flow with 4 separated streams directed to a vertical surface.

The last stage of the analysis was the investigation of the clad chemical composition using a scanning electron microscope (SEM) with energy dispersive spectroscopy (EDS) (JSM-IT100 InTouchScope; JEOL, Ltd.).

3 DEVELOPMENT AND RESULTS

3.1 Overview

The aim of the experiment was to create stainless steel clads on vertical surfaces with no cracks, no pores, good surface quality and consistent chemical composition. To meet these requirements, many trials with different sets of parameters were conducted. A range of optical conditions were assessed within this research to achieve a suitable power density to evaluate the deposition sensitivity with respect to profile and dilution response. Research completed here using an energy density range between 67 and 161 kW/mm². The variations were for the laser power from 2.5 to 10.0 kW, for the travel speed 750 to 1500 mm/min, for the powder feed rate 20 to 80 g/min and for the carrier gas feed 4 to 10 l/min. The starting and the optimized parameter set with the respective beam diameters and resulting coverage rates are given in Table 2.

Each sample consisted of 12 to 13 tracks. The interpass temperature was monitored using thermocouples and maintained below 80°C. Ar was used as both carrier and shield against oxidation of the melting pool. The cladding was performed in the 2G (PC) horizontal position using two different inclinations of the laser head. First, the laser head was positioned downward at angle of 10° to the horizontal plane (tilting). Second, the laser head was positioned parallel to the horizontal plane and at angle of 10° in opposite to the cladding direction (leading).

3.2 Laser cladding in the 2G (PC) position using 1G (PA) parameters

During the first stage of the experiments clads were created using a HPDL beam with calculated diameter of 9.0 mm and the parameters that had ensured

TABLE 2
Parameters used in the experiments.

Cladding Parameters	Laser Power (kW)	Travel Speed (mm/min)	Powder Feed Rate (g/min)	Carrier Gas (l/min)	Calculated Beam Diameter (mm)	Cladding Position	Coverage Rate (m ² /h)
Set 1 –Parameter set for 1G cladding	5.0	1000	50	10	9	2G - tilt	0.22
Optimized Set 2	4.5	1000	30	4	7	2G - lead	0.19

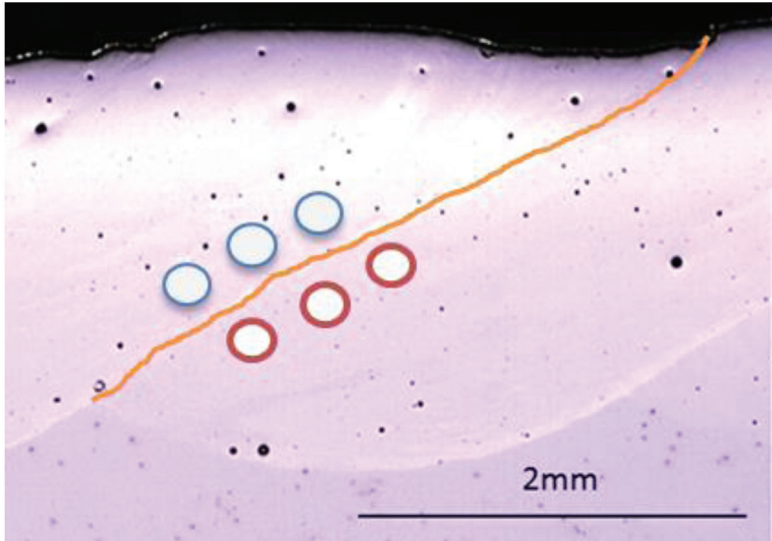
good cladding results in the downhand position using the COAX8 (IWS Fraunhofer) nozzle – cladding parameter Set 1 in Table 2; however, this parameter set was not appropriate and led to the following problems:

- (i) Bad surface quality of the clad. The clad surface was significantly rougher compared to the clad created with the same set of the parameters but in 1G (PA) flat position using the COAX8 nozzle (nozzle design for cladding in the downhand position);
- (ii) Excessive penetration depth. The penetration depth is the distance between the original surface of the substrate and the fusion line. It indicates how much of the substrate material has been melted and was alloyed with the clad material. The optimum penetration depth is potentially in the range from 100 to 200 μm since with this amount of penetration a reliable fusion can be achieved while the dilution remains limited. The average penetration depth of this particular clad (calculated from 4th to 12th track) was approximately 750 μm and therefore far too deep. Figure 3 demonstrates this where the penetration depth is indicated by the two horizontal lines;
- (iii) Variation of the clad hardness. Microhardness tests highlight another problem with this parameter set. In cladding, every clad is overlapped by the following bead creating an overlap line which indicates the melted area of the last bead. It was observed that above and below the overlap line the hardness was different. Figure 4 shows a region with overlapped beads where the overlap line is indicated. As obvious by the size of the indents (see Figure 4(b)) the hardness above the overlap line is lower (approximately 220 HV) than below the line (300 to 400 HV) which is the expected value for this material (blue dots indents). A hardness around 220 HV is typical for stainless steel, while the hardness below the overlap line is too high for this material. A hardness map was subsequently created to determine the hardness distribution. Over one thousand indents were taken with the distance between each indents of 100 μm . The results were transferred to an Excel sheet (see Figure 5). The red colour reflects the hardness of 300 HV and above, while the green colour indicates hardness below 240 HV. It is noteworthy that just below the overlap lines very high hardness values were measured which are atypi-

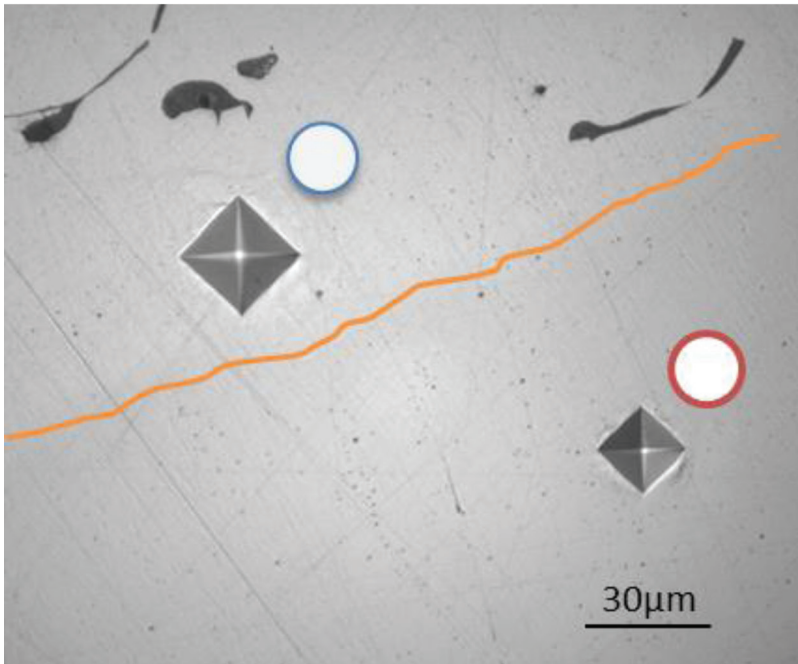


FIGURE 3

Optical micrograph of the cross-section of a clad created in the 2G position using the downhand cladding parameters of Set 1.



(a)



(b)

FIGURE 4
Optical micrographs of the cross-section of the overlap region of a clad (Set 1): (a) overview; and (b) detail. The indents are indicated by spots and the overlap by a line.

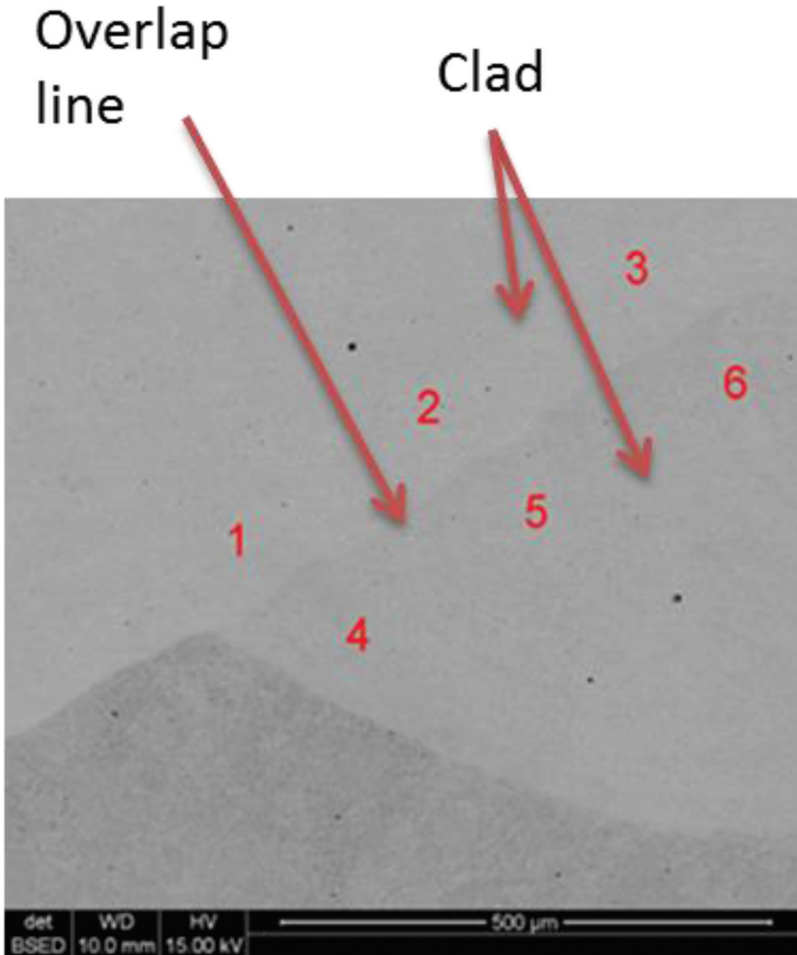


FIGURE 6
SEM micrograph showing the points of chemical composition measurements at the clad (Set 1).

TABLE 3
Composition of the clad created using parameter Set 1 (wt.%).

Element	Point 1	Point 2	Point 3	Point 4	Point 5	Point 6
Si	0.46	0.46	0.45	0.30	0.26	0.39
Mo	1.84	1.82	1.89	0.65	0.84	0.97
Cr	15.86	15.17	15.37	4.45	6.89	8.88
Mn	0.86	0.81	0.94	0.73	0.91	0.94
Fe	72.59	73.53	72.5	91.6	87.47	83.9
Ni	8.40	8.21	8.86	2.27	3.63	4.91

TABLE 4
Chemical composition of an oxide inclusion
(Set 1) determined by EDS (wt.%).

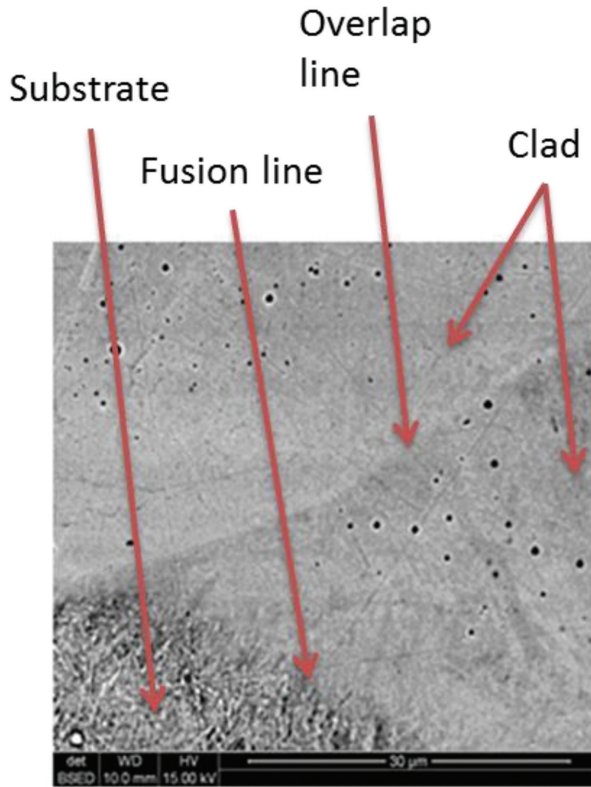
Element	Amount
O	41.62
Al	3.40
Si	19.20
Cr	7.98
Mn	23.89
Fe	3.92

3.3 Parameter optimization

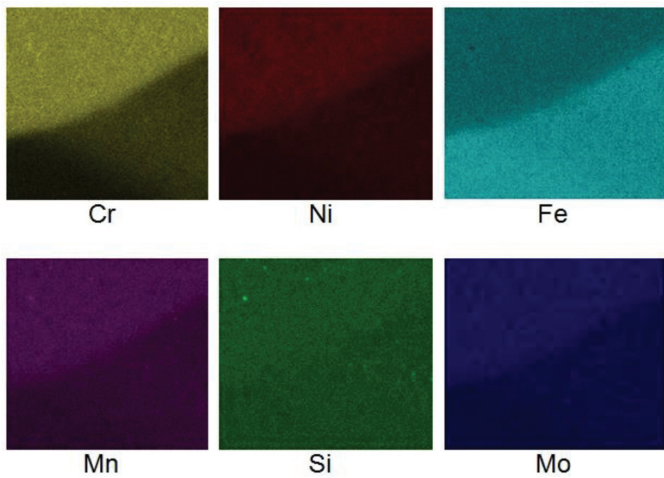
In order to overcome the described issues, an in-depth optimization process varying laser power, spot size, travel speed, powder feed rate, transport gas rate and tilt orientation has been performed. Certain combinations have resulted in lack of fusion, others to extensive penetration depth. While the influence of laser power, travel speed, and powder feed rate was as expected, the finding that transport gas rate is a key process parameter was not predicted. The reduction of transport gas significantly increases the lift, indicating a remarkable increase in powder efficiency. The final optimized parameter Set 2 is given in Table 2.

Figure 10 shows a cross section of the clad created using the optimized parameter Set 2. The clad lift is around 1.8 mm. The problems presented by cladding using Set 1 parameters have been resolved:

- (i) Surface quality. The surface of the clad is smoother and less wavy compared with the surface of the sample created using parameter Set 1;
- (ii) Penetration depth. The specimen created using the optimized parameter Set 2 has a penetration depth of approximately 150 μm (average value measured starting from the 4th bead). This is a good value that ensures limited dilution. Neither lack of fusion nor oxide inclusions have been found within the clad specimen (see Figure 10);
- (iii) Hardness of the clad. The hardness of the clad is constant and independent on the area of measurement. In the whole cross section of the specimen – above and below the overlap area, the clad hardness is in range of 220 to 240 HV (see Figure 11); and
- (iv) Chemical composition of the clad. Decreasing the carrier gas, changing the laser head angle to a leading position, and optimization of the other cladding parameters solved the issue of the high level of dilution. A constant chemical composition was present within the whole of the clad material, independently of the area of measurement. Results from the



(a)



(b)

FIGURE 7

(a) SEM micrograph of the surface of the clad produced with Set 1; and (b) EDS map showing the quantity of the alloying elements in the clad produced with Set 2.

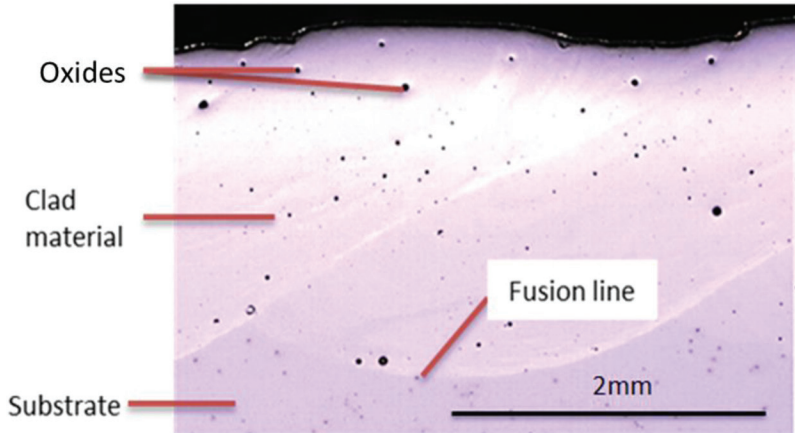


FIGURE 8

Optical micrograph of the cross-section showing oxide inclusions in the clad (Set 1). Faint speckles in the clad and substrate region are probably sample preparation artefacts.

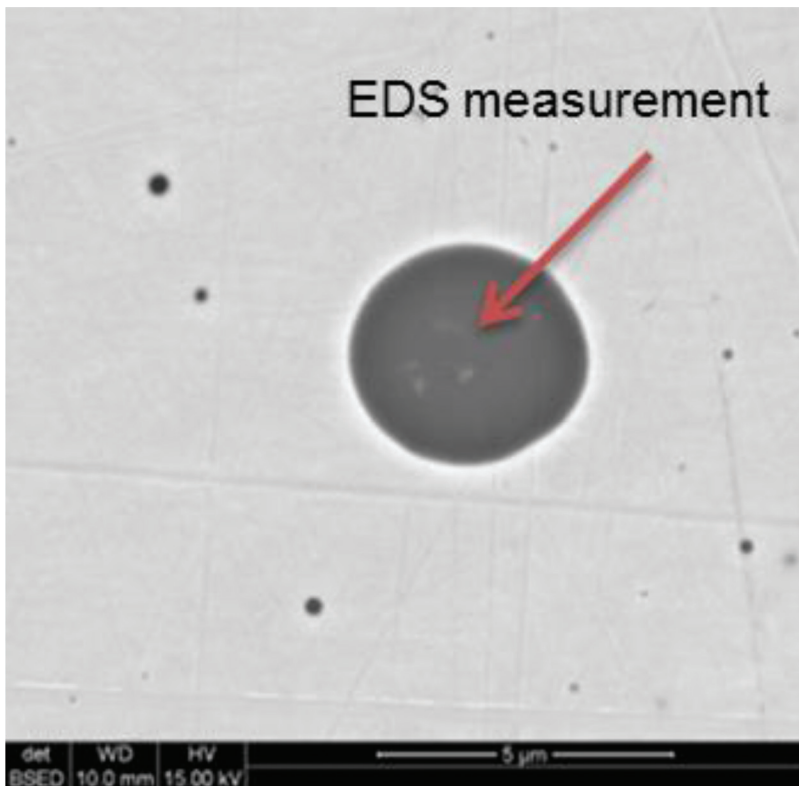


FIGURE 9

SEM micrograph showing an example of the oxide inclusion in the clad material (Set 1).



FIGURE 10

Optical micrograph view of the cross-section of the clad created using the optimized Set 2 (including several microhardness test fields).

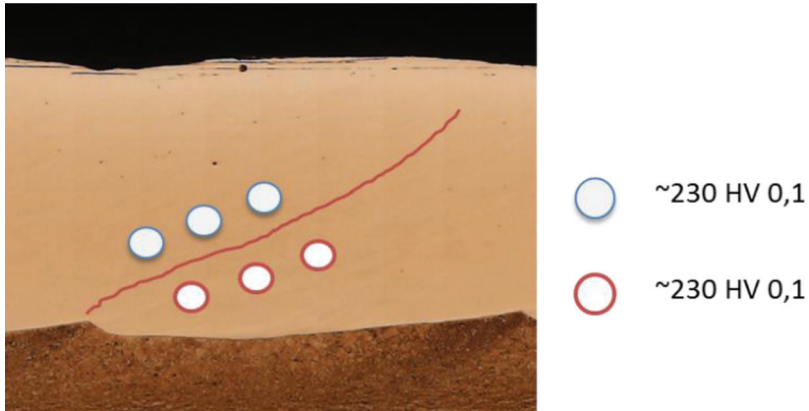


FIGURE 11

Optical micrograph of the cross-section of the clad created using the optimized parameter Set 2 with marked overlap line and area of hardness measurements.

EDS measurements are given in Figure 13 and Table 5. The points of measurement for Table 5 reported in Figure 12.

4 DISCUSSION

Laser cladding is a process in which a slight change of one of the parameters may affect the whole result very strongly. The main key process parameters (KPVs) usually considered are: laser power, travel speed and powder feed rate; however, there are more variables that may have a significant impact on the process than these. Parameters that on first look may have minor relevance, are the carrier gas flow rate and the nozzle orientation. The extensive optimization trials demonstrated the impact of carrier gas flow. When the carrier gas flow rate was decreased by 60% and the other parameters remained the same, no oxide inclusions developed, the penetration depth reduced significantly, the clad lift increased by around 30% and inter-run lack of fusion occurred. Also the change of nozzle orientation, from downhand tilting to leading, resulted to reduced penetration depth and to inter-run lack of fusion.

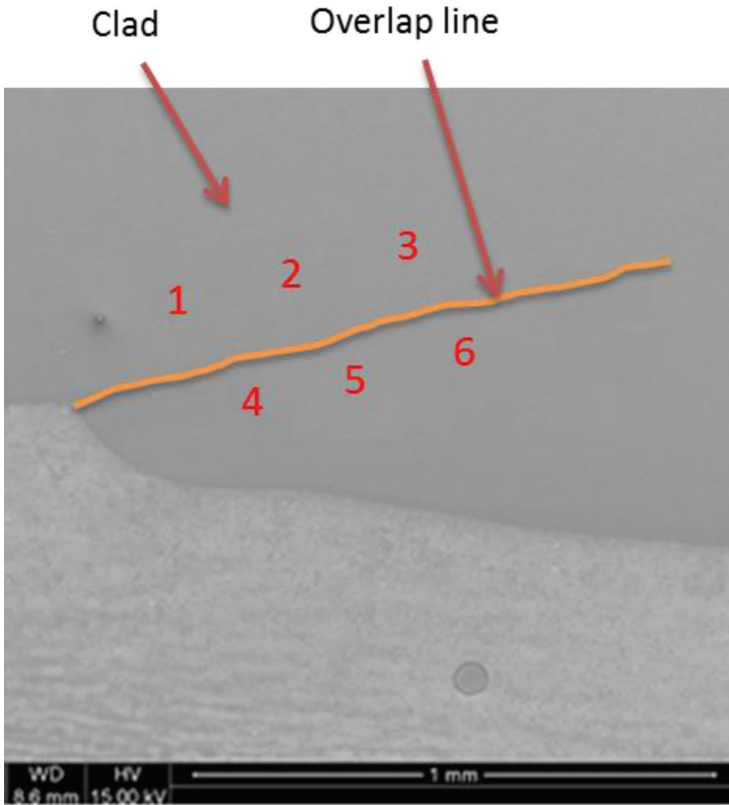
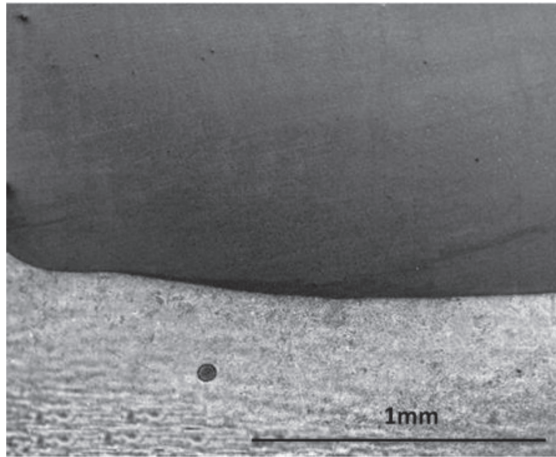


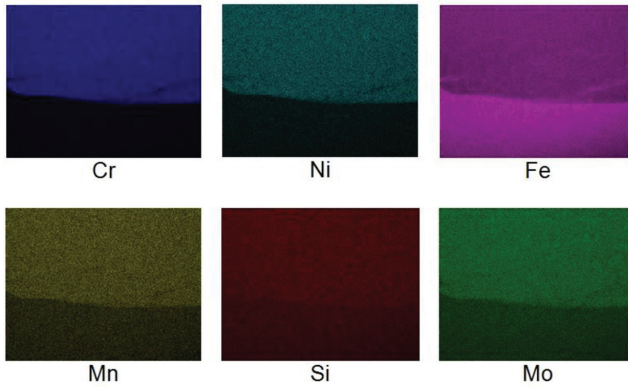
FIGURE 12
SEM micrographs showing the points of chemical composition measurements on the clad (Set 2) reported in Table 5.

The extensive penetration and dilution in the case of parameter Set 1 is the reason for the variation in chemical composition and hardness from above and below the overlap line. Due to the high level of dilution, liquid material was pulled from the substrate into the clad causing a great change in chemical composition.

Figure 14 and Figure 15 show the calculated locations within a Schaeffler diagram. For parameter Set 1 the Ni-Cr equivalent location for the area below the overlap line is within the martensite phase (*cf.* Figure 14, indication a)), while for the one above the overlap lines is within the austenite/ferrite/martensite region (*cf.* Figure 14, indication b)). The formation of a mainly martensite region below the overlap line in the case of parameter Set 1 may explain the high hardness in the range of 320 to 420 HV. For parameter Set 2 the composition above and below the overlap line are very similar and within the austenite/ferrite region (see Figure 15(a) and Figure 15(b)); hence, the hardness is also similar with a value typical of stainless steel.



a



(b)

FIGURE 13

(a) SEM micrograph of the surface of the clad produced with Set 2; and (b) EDS map showing the quantity of the alloying elements in the clad produced with Set 2.

TABLE 5

Quantity of alloying elements of the clad created using optimized parameters. Points as indicated in Figure 12.

Element	Point 1	Point 2	Point 3	Point 4	Point 5	Point 6
Si	0.59	0.74	0.57	0.49	0.59	0.75
Mo	1.90	2.32	2.08	1.93	2.29	2.10
Cr	17.43	17.31	17.88	16.43	17.46	16.82
Mn	0.94	1.13	1.46	1.04	1.14	1.31
Fe	68.98	68.63	68.37	70.82	69.15	69.53
Ni	9.54	9.54	10.59	9.30	9.27	9.49

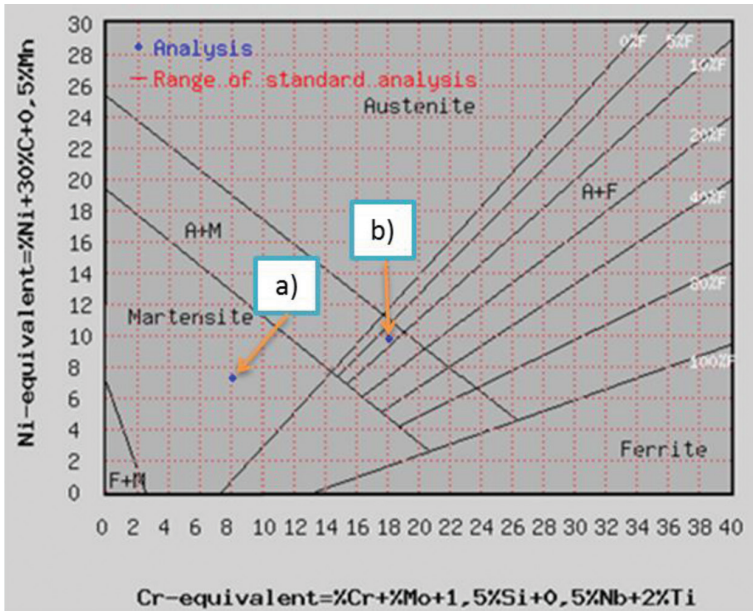


FIGURE 14

Schaeffler diagram with calculated locations of the phase composition of Set 1. Indication a) below the overlap line; indication b) above the overlap line (11).

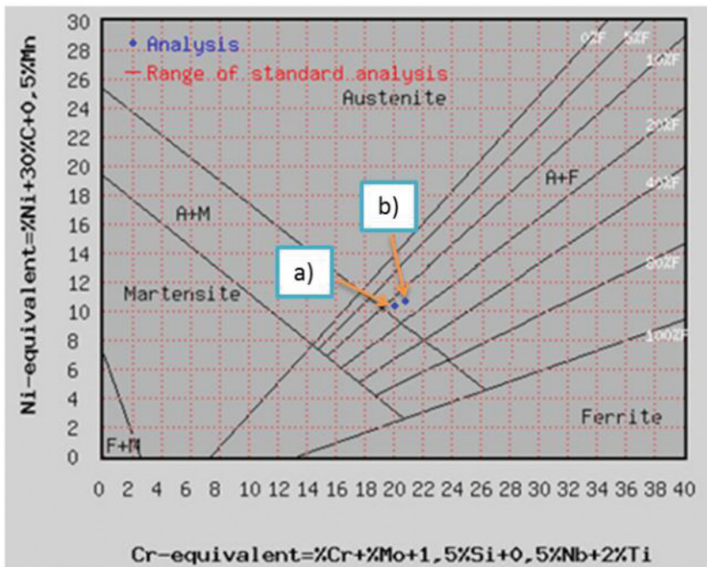


FIGURE 15

Schaeffler diagram with calculated locations of the phase composition off the optimized Set 2. Indication a) below the overlap line; indication b) above the overlap line [11].

5 CONCLUSIONS

The following conclusions are related to the laser cladding process in 2G (PC) horizontal position using a COAX12 powder nozzle and have been developed based on the experimental results as well as on the discussion above:

- (i) The change of the position of the cladded surface, from flat to horizontal, affects the cladding process. This is because gravity affects the powder stream and weld pool in a different way;
- (ii) It is possible to achieve high quality, stainless steel clads on vertical walls (optimum dilution and penetration depth, smooth surface, no internal and external defects);
- (iii) The carrier gas flow rate is one important cladding parameter that has influence on the following aspects: efficiency of the cladding process; penetration depth and dilution; and occurrence of oxide inclusions; and
- (iv) The nozzle orientation (tilting against leading) has influence on the following aspects: penetration depth and dilution; and clad smoothness (waviness).

The optimized parameter Set 2 enables the introduction of cladding in 2G horizontal position for large components. This has a major impact on manufacturing costs and safety issues since complex component manipulation will be made redundant. The introduction of this novel technology may have the potential to reduce drastically production costs.

ACKNOWLEDGMENTS

The authors wish to acknowledge the UK High Value Manufacturing Catalyst for sponsoring this project. The authors are also indebted to Stephen Bloomer (Nuclear AMRC) and Holger Hillig (IWS Fraunhofer) for their experimental work and advice.

REFERENCES

- [1] Khanna A.S., Kumari S., Kanungo S. and Gasser A. Hard coatings based on thermal spray and laser cladding. *International Journal of Refractory Metals and Hard Materials* **27**(2) (2009), 485–491.
- [2] Vilar R. Laser cladding. *Journal of Laser Applications* **11**(2) (1999), 64–79.
- [3] Robinson A. and Bonell S. Longer life with welded claddings. *World Pumps* **2010**(9) (2010), 42–45.
- [4] Kathuria Y.P. Some aspects of laser surface cladding in the turbine industry. *Surface & Coatings Technology* **132**(2–3) (2000), 262–269.

- [5] Goodwin P. Laser cladding of industrial components. *Industrial Laser Application Symposium 2015 (ILAS 2015)*. 17-18 March 2015, Kenilworth, UK. pp. 126–132.
- [6] Weisheit A., Backes G., Stromeyer R., Gasser A., Wissenbach K. and Poprawe R. Powder injection: The key to reconditioning and generating components using laser cladding. *Materials Week 2001, International Congress on Advanced Materials, their Processes and Applications*. 1-4 October 2001, Munich, Germany. p. 8.
- [7] Baufeld B. and Lawler S. Laser cladding of large scale parts at the Nuclear AMRC. *9th International Laser Symposium*. 24 February 2016, Dresden, Germany. pp. 12–23.
- [8] ASME Boiler & Pressure Vessel Code IX QW-460 (2013), *ASME. IX: The American Society of Mechanical Engineers*.
- [9] CLA (2016). *Nozzle Technology COAX12*. Retrieved 8th January 2017, from http://www.cla.fraunhofer.org/en/products/coax_12.html 2017
- [10] IWS (2017). *Modular powder nozzle system COAXn*. Retrieved 8th January 2017, from http://www.iws.fraunhofer.de/en/business_fields/surface_treatment/laser_cladding/system_technology/COAXn.html 2017
- [11] migalco.com (2016). *Schaeffler Diagram*. Retrieved 8th January 2047, from <http://www.migweld.de/english/service/welding-stainless-steels/schaeffler-diagram-for-standard-analysis/>